AD-A041 177 NAVAL RESEARCH LAB WASHINGTON D C F/G 20/9
INTERACTION OF ELECTROMAGNETIC WAVES WITH A MOVING IONIZATION F--ETC(U)
JUN 77 M LAMPE, E OTT
UNCLASSIFIED NRL-MR-3531 NL

1 OF 1
AD A041177

END
DATE FILMED
7-77

NRL Memorandum Report 3531

Interaction of Electromagnetic Waves with a Moving Ionization Front

MARTIN LAMPE

Plasma Dynamics Branch
Plasma Physics Division

EDWARD OTT

Department of Electrical Engineering
Cornell University
Ithaca, New York 14853

June 1977

NAVAL RESEARCH LABORATORY
Washington, D.C.

SECURITY CLASSIFICATION OF THIS PAGE (When Data Entered)

REPORT DOCUMENTATION PAGE		READ INSTRUCTIONS BEFORE COMPLETING FORM
1. REPORT NUMBER NRL Memorandum Report 3531	2. GOVT ACCESSION NO.	3. RECIPIENT'S CATALOG NUMBER
4. TITLE (and Subtitle) INTERACTION OF ELECTROMAGNETIC WAVES WITH A MOVING IONIZATION FRONT		5. TYPE OF REPORT & PERIOD COVERED Interim report on a continuing NRL problem. 6. PERFORMING ORG. REPORT NUMBER
7. AUTHOR(s) Martin Lampe (NRL) and Edward Ott (Cornell University)		8. CONTRACT OR GRANT NUMBER(s) NRL-MR-3531
9. PERFORMING ORGANIZATION NAME AND ADDRESS Naval Research Laboratory Washington, D.C. 20375		10. PROGRAM ELEMENT, PROJECT, TASK AREA & WORK UNIT NUMBERS NRL Problem R08-93B Project N60921-76-WR-W0263
11. CONTROLLING OFFICE NAME AND ADDRESS Naval Surface Weapons Center Silver Spring, Maryland 20910		12. REPORT DATE June 1977 13. NUMBER OF PAGES 58
14. MONITORING AGENCY NAME & ADDRESS (if different from Controlling Office)		15. SECURITY CLASS. (of this report) UNCLASSIFIED 15a. DECLASSIFICATION/DOWNGRADING SCHEDULE

16. DISTRIBUTION STATEMENT (of this Report)

Approved for public release; distribution unlimited.

17. DISTRIBUTION STATEMENT (of the abstract entered in Block 20, if different from Report)

18. SUPPLEMENTARY NOTES

19. KEY WORDS (Continue on reverse side if necessary and identify by block number)

Submillimeter waves
Millimeter reflection
Ionization front scattering
Microwave upshift
Microwave reflection

20. ABSTRACT (Continue on reverse side if necessary and identify by block number)

This paper considers the problem of an electromagnetic wave packet incident on a relativistically moving plane ionization or recombination front separating a stationary neutral gas region from a stationary plasma region. The frequency of the reflected wave packet is found to obey the usual double Doppler shift relation. However, the reflection coefficients and the physics can differ significantly from the case of reflection from moving material objects. The ratio of the energy in the incident wave packet is shown to be at most (i.e. for the overdense case) ω_i^*/ω_r^* for the ionization

(Continues)

DD FORM 1 JAN 73 1473 EDITION OF 1 NOV 65 IS OBSOLETE S/N 0102-014-6601

SECURITY CLASSIFICATION OF THIS PAGE (When Data Entered)

20. Abstract (Continued)

front ($\omega_i^* < \omega_r^*$), and ω_r^*/ω_i^* for the recombination front ($\omega_i^* > \omega_r^*$), where ω_i^* and ω_r^* are the incident and reflected wave frequencies in the laboratory frame. These results have important implications for the production of submillimeter wavelength pulses by upshifted reflection from a relativistically moving ionization front.

CONTENTS

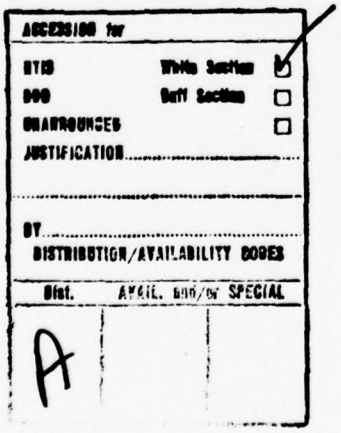

INTERACTION OF ELECTROMAGNETIC WAVES WITH A MOVING IONIZATION FRONT

I. Introduction

The refractive index non-uniformity at the edge of a plasma can act as a mirror, reflecting incident electromagnetic waves. If the plasma edge is moving at velocity U, the reflected wave will be doubly Doppler shifted,[1] so that its frequency[2] ω_r^* is related to the incident frequency ω_i^* by

$$\frac{\omega_r^*}{\omega_i^*} = \frac{1 + \beta \cos \theta_i^*}{1 - \beta \cos \theta_r^*} , \tag{1}$$

where $\beta \equiv U/c$ and θ_i^*, θ_r^* are the angles of incidence and reflection.[3] Furthermore, a similar Doppler relation occurs between the duration of the reflected pulse τ_r^* and that of the incident pulse τ_i^*,

$$\frac{\tau_r^*}{\tau_i^*} = \frac{\omega_i^*}{\omega_r^*} . \tag{2}$$

Equation (2) applies in free space; the situation in a waveguide is somewhat different and will be discussed later. Thus an upshifted wave pulse will also be compressed, which tends to increase the peak reflected power.

Granatstein, et al.,[3] in a recent experiment, have taken advantage of this phenomenon to produce intense pulses of 8mm radiation by reflecting an incident 3.2 cm microwave pulse off the front of a high-current relativistic electron beam, which plays the role of the overdense plasma.[4] This experiment is part of a recent surge of

Note: Manuscript submitted May 23, 1977.

interest in the exploitation of advances in relativistic electron beam technology to generate intense millimeter and submillimeter radiation.[5] However, we pointed out recently[6] that the plasma itself need not be moving, for the wave reflected off the plasma edge to be Doppler shifted. It is only necessary that the boundary between the plasma and the surrounding neutral medium be moving. Thus an alternative method for upshifting a microwave beam is to reflect it from a moving ionization or recombination front in a stationary gas, i.e. a moving interface between regions where the gas (stationary in the laboratory frame) is unionized and ionized. (In the case of an ionization front, the interface moves toward the neutral gas, $U > 0$; a recombination front moves toward the plasma, $U < 0$.) In Ref. 6 we proposed that this might be a practical method of generating millimeter and submillimeter radiation and presented preliminary theoretical calculations of the process. In the present paper, these are extended to a detailed and comprehensive theory. Throughout this paper, the plasma is treated as a cold and collisionless fluid. Also the theory is linear in the amplitude of the electromagnetic wave, so that no scattering processes other than refractive index variation are considered. Except for these assumptions, the theory is quite general, and no mathematical approximations are needed.

In Section II we treat the case of a wave incident normally on a sharp, infinite planar, moving ionization or recombination front (i.e. a discontinuity in the electron density). This is the simplest case to understand. In Section IIA the reflection coefficient is calculated exactly. It is demonstrated that the Doppler shift and reflected pulse

duration are given by Eqs. (1) and (2) with $\theta_i^* = \theta_r^* = 0$, the same as for a moving plasma,[3] but in other respects reflection off a moving ionization front differs significantly from reflection off a moving plasma. A moving overdense plasma (the underdense case is also treated in Sec. II, but will not be discussed in this introduction), acts as a perfect moving mirror, reflecting and upshifting each photon. Thus, according to Eqs. (1) and (2), the energy ϵ_r^* and power P_r^* of the reflected pulse are related to the incident ϵ_i^* and P_i^* by

$$\epsilon_r^*/\epsilon_i^* = \omega_r^*/\omega_i^*, \tag{3}$$

$$P_r^*/P_i^* = (\omega_r^*/\omega_i^*)^2 \tag{4}$$

Equations (3) or (4) hold for either an oncoming or receding "mirror". For an oncoming mirror ϵ_r^* exceeds ϵ_i^*, with the extra energy being supplied by the kinetic energy of the moving plasma; for the receding mirror, energy is absorbed by the recoiling mirror. However, a moving ionization front in a stationary plasma has no kinetic energy to share with the wave; consequently, one must have $\epsilon_r^* \leq \epsilon_i^*$. The complete calculation does indeed show that this is true. Furthermore, the physical processes at work are shown to be different for the case of an oncoming ionization front ($U > 0$, $\beta > 0$), as opposed to a receding recombination front ($U < 0$, $\beta < 0$). Therefore $\epsilon_r^*/\epsilon_i^*$ and P_r^*/P_i^* cannot be represented by a single analytic expression valid for both $U > 0$ and $U < 0$, as in Eqs. (1-4). We find that Eqs. (3,4) hold for a recombination front but that for an ionization front,

$$\epsilon_r^*/\epsilon_i^* = \omega_i^*/\omega_r^*, \tag{5}$$

$$p_r^*/p_i^* = 1. \tag{6}$$

The difference between the cases $U < 0$ and $U > 0$ is explained in terms of the excitation in the latter case of a third normal mode in the plasma, in addition to the usual evanescent and growing electromagnetic modes. The existence of this third wave has not been previously recognized.

In Section IIB it is demonstrated explicitly that the reflection and transmission coefficients satisfy energy conservation. These calculations enhance physical understanding and help to dispel confusion about this reflection process. In particular, it is shown that the mechanism which ionizes the gas plays no role in the wave energetics, and that (unlike the case of scattering off a moving plasma) no energy is exchanged between the wave and the plasma recoil. Wave energy is, however, deposited in the kinetic and magnetic energy associated with stationary transverse electron currents that are set up in the plasma as a result of the reflection process.

In Section IIC, the case of an oncoming front moving faster than the speed of light is treated. Such a front is physically realizable, but paradoxes are avoided, as it is shown that no wave reflection occurs.

In Section III the reflection problem is formulated and solved with no restriction on the shape or width of the electron density profile in the ionization front (but still for the case of normal incidence on an infinite planar front). It is shown that, in the overdense case,

Eqs. (1)-(4) for $U < 0$, and (1), (2), (5), (6) for $U > 0$, hold quite generally. In the underdense case, explicit solutions for the reflection coefficient are written in terms of the reflection coefficient for a stationary electron density profile of the same shape, in a stationary plasma. In Section IIIB, a complete and explicit solution is found for a particular electron density profile in the front (hyperbolic tangent), whose width can be varied from zero to infinity. In Section IIIC, energy conservation is demonstrated and discussed for the limiting case of a broad front, based on a WKB calculation.[7]

In Section IV, the theory is extended to electromagnetic waves propagating in a waveguide, and to waves obliquely incident on the front in free space.

A considerable theoretical literature exists on reflection at moving discontinuities in material properties,[8-15] most of which is incorrect <u>when applied to plasma ionization fronts</u>. In Section V, we briefly comment on this literature, and discuss in some detail the macroscopic model of electromagnetic scattering at a moving discontinuity in the dielectric coefficient of a stationary dielectric.[12] It is shown that (contrary to some claims in the literature[13,14]) this model is inapplicable to moving ionization fronts, and is, in fact, only one of several possible models for a discontinuity in a dielectric. These models, which lead to different reflection coefficients, must be sorted out on the basis of the microscopic physics.

In Section VI, we discuss the technological applications of the ionization front scattering process.

Section VII summarizes our results.

II. Sharp Ionization or Recombination Front

A. Solution of the Scattering Problem

We shall perform our calculation in the frame of reference in which the ionization or recombination front is stationary (the "front frame").[2] In this frame, in the ionization front case, neutral gas flows into the discontinuity from the left at velocity $U > 0$, and plasma flows away to the right at the same[16] velocity U, as illustrated in Fig. 1. In the case of a recombination front, the only difference is that $U < 0$, i.e. plasma flows into the front and gas flows out. In the front frame, the scattering problem is stationary and thus an incident wave of frequency ω generates reflected and transmitted waves at the same frequency. We shall assume throughout this paper, for convenience, that the neutral gas has the dielectric properties of the vacuum. In the present section, we assume that the front is much narrower than the wavelength of any wave, so that the electron density $n(z)$ in Fig. 1 can be represented as a step function, discontinuous at the front. In Section III we shall consider the general case where $n(z)$ is arbitrary.

We first solve for the transverse normal modes in the plasma, where the electron density n is constant. The transverse electron velocity $\underset{\sim}{y}$ in the presence of the transverse wave fields $\underset{\sim}{E}$ and $\underset{\sim}{B}$ is determined by the linearized momentum conservation equation (i.e. generalized Ohm's law),

$$\frac{\partial \underset{\sim}{v}}{\partial t} + U \frac{\partial \underset{\sim}{v}}{\partial z} = - \frac{e}{m_e \gamma} \left(\underset{\sim}{E} + \frac{1}{c} \underset{\sim}{U} \times \underset{\sim}{B} \right) \tag{7}$$

In Eq. (7), $\gamma \equiv (1 - \beta^2)^{-1/2}$. Also, using Maxwell's equations and neglecting the perturbed ion velocity,

$$\nabla \times \underset{\sim}{E} = - \frac{1}{c} \frac{\partial \underset{\sim}{B}}{\partial t} , \tag{8}$$

$$\nabla \times \underset{\sim}{B} = \frac{1}{c} \frac{\partial \underset{\sim}{E}}{\partial t} - \frac{4\pi}{c} ne \underset{\sim}{v} \tag{9}$$

and assuming spatial and temporal dependence $\exp(ikz - i\omega t)$, Eqs. (7)-(9) lead to the dispersion relation

$$\left(k^2 - \frac{\omega^2 - \omega_p^2}{c^2} \right) \left(k - \frac{\omega}{U} \right) = 0, \tag{10}$$

where $\omega_p^2 \equiv 4 \pi ne^2/m_e \gamma$. Thus there are three normal modes at any given frequency ω,

$$k_1(\omega) = \begin{cases} \frac{\omega}{c} \left(1 - \frac{\omega_p^2}{\omega^2} \right)^{1/2} , & \text{if } \omega^2 > \omega_p^2 \\ i \frac{\omega}{c} \left(\frac{\omega_p^2}{\omega^2} - 1 \right)^{1/2} , & \text{if } \omega^2 < \omega_p^2 , \end{cases} \tag{11a}$$

$$k_2(\omega) = - k_1(\omega), \tag{11b}$$

$$k_m(\omega) = \omega/U . \tag{11c}$$

The roots k_1 and k_2 are just the usual rightward- and leftward-propagating electromagnetic waves if the plasma is underdense, i.e. $\omega_p < \omega$, or the equally well-known evanescent and growing waves if the

plasma is overdense, i.e. $\omega_p > \omega$. We note that the dispersion relation for electromagnetic waves is covariant in the form

$$\omega_p^2 = \omega^2 - k^2c^2. \tag{12}$$

It follows that ω_p is a scalar under Lorentz transformation, and thus is numerically equal to its value in the laboratory frame, $\omega_p^* = (4\pi n^* e^2/m_e)^{1/2}$. Hence, in the laboratory frame, the condition for the plasma to be overdense is

$$\omega_p^* > \omega_i^* \left(\frac{1+\beta}{1-\beta}\right)^{1/2} = \omega. \tag{13}$$

The other normal mode, k_m, is often overlooked in discussions of transverse waves in plasmas. The nature of this wave is elucidated by noting that $E_m = (\omega/kc)B_m = \beta B_m$, so that if we Lorentz transform to the laboratory frame, where the plasma is stationary, we find $E_m^* = \omega_m^* = 0$. Thus in the laboratory frame this "wave" is just a cold stationary magnetic disturbance with $\underset{\sim}{B}_m^* = \underset{\sim}{B}_o e^{ik^*z}$ and $\underset{\sim}{J}_m^* = ik^*\hat{z}\times\underset{\sim}{B}_o e^{ik^*z}$, which is indeed a solution of Maxwell's equations and the linearized fluid equation of motion, and is therefore a permissible mode in a cold collisionless plasma. In a frame where the plasma is streaming, this mode becomes a genuine undamped, dispersionless electromagnetic wave, carrying energy and momentum and propagating at the plasma streaming velocity.

The following argument illustrates why the magnetic wave is excited at the sharp ionization front. An electron moving in the plasma region, in the presence of the evanescent wave (we assume,

for the moment, that the plasma is overdense), obeys the equation of motion

$$-\frac{d\underset{\sim}{v}}{dt} = \frac{e}{m_e}\left(\underset{\sim}{E} + \frac{1}{c}\underset{\sim}{U} \times \underset{\sim}{B}\right) = \frac{e}{m_e}\underset{\sim}{E}(x = 0,\ t = 0)\left(1 - \frac{kU}{\omega}\right)e^{i(kz-\omega t)}. \quad (14)$$

Integrating back over an electron's orbit, and imposing the initial condition that the electron is born (ionized), at $z = z'$ and time $t-(z-z')/U$, with zero velocity in the laboratory frame,

$$\underset{\sim}{v}[z',\ t-(z-z')/U] = 0, \quad (15)$$

we find

$$\underset{\sim}{v}(z,t) = \frac{ie\underset{\sim}{E}(0,0)}{m_e\omega}\left\{\exp i(kz-\omega t) - \exp\left[-i\omega\left(t-\frac{z-z'}{U}\right)\right]\right\}. \quad (16)$$

Since, in the case of a sharp ionization front at $z' = 0$, <u>all</u> electrons are born at $z' = 0$, the current $\underset{\sim}{J}$ is given by $\underset{\sim}{J} = -ne\underset{\sim}{v}$, with $\underset{\sim}{v}$ given in Eq. (16). The first term in Eq. (16) leads to the current associated with the evanescent wave, while the second term is the source of the magnetic wave, and is associated with the boundary condition of a sharp ionization front.

We now set about matching waves at the vacuum-plasma interface, to determine the reflection and transmission coefficients. We shall see that the physics is different for an advancing ionization front ($U > 0$) and for a retreating recombination front. We treat the case $U > 0$ first.

Equations (11) indicate that there are three possible waves in the plasma at frequency ω, but the wave k_2 is ruled out by its unphysical behavior at $x = +\infty$, since it is growing if the plasma is overdense, or leftward-propagating if the plasma is underdense. Thus at the interface, we must match four waves, the incoming wave (of known amplitude), the reflected wave in the gas, and two plasma waves, k_1 and k_m. Thus there are three unknown amplitudes (one more than in the usual dielectric interface problem), and we need three matching conditions. It is immediately clear from integrating Maxwell's equations (8,9) across the interface, that continuity of E and B are required, as usual. A third condition is supplied by noting that electrons are born (by ionization) at the interface with transverse velocity $\underset{\sim}{y} = 0$, and then stream away into the plasma at axial velocity U, while they begin to oscillate in the perpendicular plane. Thus the current at the interface is

$$\underset{\sim}{J}(z = 0) = -ne\underset{\sim}{y}(z = 0) = 0, \tag{17}$$

so that $\underset{\sim}{J}$ is continuous across the interface. Equation (9) thus indicates that $\frac{\partial B}{\partial z}$ is also continuous across the interface.

By noting that

$$B = (kc/\omega)E, \tag{18a}$$

and

$$(\partial B/\partial z) = (ik^2c/\omega)E, \tag{18b}$$

using Eqs. (11) for the plasma waves and $k_i = \omega/c$, $k_r = -\omega/c$ for the incident and reflected vacuum waves, we can write the matching conditions,

$$E_i = -E_r + E_m + E_1, \tag{19a}$$

$$E_i = E_r + \beta^{-1} E_m + WE_1, \tag{19b}$$

$$E_i = -E_r + \beta^{-2} E_m + W^2 E_1, \tag{19c}$$

where

$$W \equiv \frac{k_1 c}{\omega} = \begin{cases} (1 - \omega_p^2/\omega^2)^{1/2}, & \text{if } \omega^2 > \omega_p^2 \quad (20a) \\ i(\omega_p^2/\omega^2 - 1)^{1/2}, & \text{if } \omega^2 < \omega_p^2. \quad (20b) \end{cases}$$

The solution of Eqs. (19) for the amplitudes of the reflected and magnetic waves are

$$\frac{E_r}{E_i} = \frac{1-\beta}{1+\beta} \quad \frac{1-W}{1+W}, \tag{21a}$$

$$\frac{E_m}{E_i} = \frac{2\beta^2(1-W)}{(1+\beta)(1-\beta W)}. \tag{21b}$$

The magnetic field amplitudes of each of the waves are determined by (21) and (18a) and we can then write down the electromagnetic energy flux (i.e. Poynting power) P, for each wave:

$$\frac{P_r}{P_i} = |\Gamma|^2 \left(\frac{1-\beta}{1+\beta}\right)^2, \tag{22a}$$

$$\frac{P_m}{P_i} = \frac{4\beta^4}{(1+\beta)^2} \left|\frac{1-W}{1-\beta W}\right|, \tag{22b}$$

where

$$\Gamma = \frac{1-W}{1+W} \tag{23}$$

is the (amplitude) reflection coefficient for a stationary sharp ionization front. For the overdense case, $|\Gamma| = 1$. We also note, for use in the next section, the zz components of the momentum flux, $F \equiv - < E^2 + B^2 > /8\pi$, for each wave (where the brackets indicate a time average):

$$F_r = P_r/c, \tag{24a}$$

$$F_m = \frac{\beta^2(1+\beta^2)}{(1+\beta)^2} \quad \frac{1}{\beta^2 + (1-\beta^2)(\omega^2/\omega_p^2)} \quad \frac{E_i^2}{4\pi} . \tag{24b}$$

For simplicity, (24b) is given only for the overdense case (i.e. W imaginary).

We now transform these results back to the laboratory frame. The Doppler shift in going from the front frame to the laboratory frame is

$$\begin{aligned} \omega_r^* &= \omega\gamma(1+\beta), \\ \omega_i^* &= \omega\gamma(1-\beta), \end{aligned} \tag{25}$$

so that

$$\frac{\omega_r^*}{\omega_i^*} = \frac{1+\beta}{1-\beta} . \tag{26}$$

Since the number of photons in the incident wave packet, or in the reflected wave packet, is frame-independent, the wave packet energy transforms as

$$\epsilon_i^* = \epsilon_i \gamma(1-\beta), \tag{27a}$$

$$\epsilon_r^* = \epsilon_r \gamma(1+\beta) \tag{27b}$$

Combining Eqs. (22a) and (27) gives

$$\frac{\epsilon_r^*}{\epsilon_i^*} = \frac{\omega_i^*}{\omega_r^*} |\Gamma|^2 = \frac{1-\beta}{1+\beta} |\Gamma|^2 \tag{28}$$

for the energy reflection coefficient in the laboratory frame. Finally, the pulse duration transforms as the inverse of a frequency,[17]

$$\frac{\tau_r^*}{\tau_i^*} = \frac{\omega_i^*}{\omega_r^*} , \tag{29}$$

whence the power reflection coefficient in the laboratory frame is seen to be

$$\frac{P_r^*}{P_i^*} = |\Gamma|^2. \tag{30}$$

For the overdense case, $\Gamma = 1$, and $P_r^* = P_i^*$.

We now turn our attention to the case $U < 0$, i.e. a retreating recombination front. In this case the magnetic wave is an incoming traveling wave from $+\infty$, and thus is ruled out by causality. Thus the wave k_1 (evanescent if the plasma is overdense, rightward-propagating if overdense) is the only permissible wave in the plasma, and the usual matching conditions of continuity of E and B at the interface still

hold, but the third condition, continuity of $\frac{\partial B}{\partial x}$, does not hold for this case. It derived from the fact that $J(z = 0) = 0$ for an ionization front at $z = 0$. However for a recombination front, electrons dying (by recombination) at $z = 0$ carry current at the instant of recombination, and thus $J(z = 0) \neq 0$.

Thus the matching conditions become the same as in the elementary problem of a stationary interface,

$$E_i = -E_r + E_1, \tag{31a}$$

$$E_i = +E_r + iWE_1, \tag{31b}$$

whence the coefficients of reflection and transmission are found to be

$$\frac{P_r}{P_i} = |\Gamma|^2 , \tag{32a}$$

$$\frac{P_m}{P_i} = 1-|\Gamma|^2 . \tag{32b}$$

Transforming Eqs. (32) back to the laboratory frame, exactly as in the derivation of Eqs. (28) and (30), we find

$$\frac{\epsilon^*_r}{\epsilon^*_i} = \frac{\omega^*_r}{\omega^*_i} |\Gamma|^2 = \frac{1-|\beta|}{1+|\beta|} |\Gamma|^2, \tag{33}$$

$$\frac{P^*_r}{P^*_i} = \left(\frac{\omega^*_r}{\omega^*_i}\right)^2 |\Gamma|^2 \tag{34}$$

for the coefficients of pulse energy and power reflection in the laboratory frame.

B. Energy Conservation

We shall now demonstrate that our solution conserves energy. We continue to work in the front frame of reference. We note first that we have assumed, in the linear electrodynamics calculation of Section II A, that the streaming velocity U is constant, and equal in the plasma and gas. In fact U does change across the front, since the plasma must recoil to conserve momentum, but it is consistent to neglect the recoil velocity in a linear calculation, since it is second order in the wave amplitude (and also is inversely proportional to the ion mass). However, the recoil must be included to satisfy the conservation laws (in the front frame). The situation is analogous to bouncing a light ball off a very heavy moving object (e.g. the earth): the recoil velocity of the earth is negligible, yet it absorbs the momentum change of the ball.

The recoil velocity ΔU could be calculated from a second order electrodynamic treatment (including ponderomotive force). We take the simpler point of view here that ΔU is determined by momentum conservation; we can then go on to verify that energy is also conserved. We also note that a small density change at the front is associated with the recoil, through the continuity equation. However, quasineutrality requires that the electron and ion densities be locally equal (assuming singly charged ions, for simplicity).

With this preamble, we proceed to write down the conservation equations for particles, the z-component of momentum, and energy, considering first the case $U > 0$ (ionization front):

$$0 = \Delta(nU), \tag{35a}$$

$$P_i + P_r - P_m = \Delta[nU^2(m_e\gamma_e + m_i\gamma_i)], \tag{35b}$$

$$cP_i - cP_r - F_m = \Delta[nUc^2(m_e\gamma_e + m_i\gamma_i)]. \tag{35c}$$

The terms on the left hand side of Eqs. (35b,c) are the electromagnetic momentum and energy flux, P and F respectively, for the incident, reflected, and magnetic waves, given by Eqs. (22,24). We consider here only the overdense case, in which no energy or momentum flux is associated with the evanescent wave in the plasma. On the right hand side are the changes in particle momentum and energy flux due to the presence of the waves; Δ can be interpreted as the difference in a quantity in the plasma from what it would be if there were no incident wave. The right hand side includes the changes due to both the recoil velocity ΔU, and the transverse electron oscillations associated with the magnetic wave. Thus

$$\Delta\gamma_i = \gamma^3 U\Delta U/c^2, \tag{36a}$$

$$\Delta\gamma_e = \gamma^3(U\Delta U + \tfrac{1}{2} < v^2 >)/c^2, \tag{36b}$$

where $\gamma \equiv (1-U^2/c^2)^{-1/2}$ is the unperturbed value (same for electrons and ions) and $< v^2 >$ is the mean square oscillating velocity. According to Eqs. (9) and (11a), v is given by

$$\underset{\sim}{v} = -\frac{i\omega}{4\pi ne}(-\beta^2+1)\underset{\sim}{E}. \tag{37}$$

Using the magnetic wave amplitude (21b) in (37) then gives

$$nm_e\gamma \langle v^2 \rangle = \frac{4(1-\beta)^2}{1-\beta^2+\beta^2\omega_p^2/\omega^2} \frac{E_i^2}{8\pi} . \qquad (38)$$

Solving Eqs. (35a,b) for ΔU, and substituting in Eq. (35c), verifies (after some tedious algebra) that Eq. (35c) is satisfied identically, and thus energy is conserved.

Three points concerning this energy conservation demonstration deserve comment. First, the external mechanism which causes the plasma ionization plays no role, neither contributing energy to the waves nor absorbing energy. Consistent models could in fact be constructed in which the energy associated with ionization becomes negligibly small. Secondly, part of the incident wave energy penetrates the plasma, in the form of electromagnetic and transverse electron kinetic energy associated with the magnetic wave. This occurs even though the plasma is overdense. However, the situation would look rather different in the laboratory frame, where the plasma is stationary but the ionization front is moving. Since the magnetic "wave" is stationary in this frame, one could more accurately say that energy is deposited in the plasma in the vicinity of the ionization front, and remains in the same place in the plasma as the front moves on. Thirdly, we note that energy transfer to the plasma, through the recoil, occurs in the front frame. As seen in the laboratory frame where the plasma is stationary, the plasma kinetic energy of recoil would be vanishingly small [order (ΔU^2)]. The comparison with the case of a "moving mirror", i.e. a physically moving plasma, is instructive:

here the recoiling plasma, which is moving in the laboratory frame, does exchange energy with the wave in the laboratory frame; hence the possibility that reflected wave energy exceeds incident wave energy in this case.

We shall now briefly discuss energy conservation for the recombination front case, $U < 0$. The formal framework of the calculation is similar to Eqs. (35), but it is now appropriate to consider Δ to represent the changes in quantities at the recombination front, due to the presence of the waves. In this case, the magnetic wave is absent. However, the electrons acquire a transverse velocity v, by passing through the evanescent wave en route to the recombination front. A calculation similar to that of Eq. (38) shows that just to the right of the ionization front

$$\frac{1}{2} nm_e \gamma < v^2 > = E_i^2/4\pi . \qquad (39)$$

Completing the calculation, just as in the case $U > 0$, then verifies that energy is conserved. The reflected energy in the laboratory frame is less than the incident energy; the difference goes into the electron transverse kinetic energy, Eq. (39); upon recombination, this energy either dissipates by heating the gas or goes off as recombination radiation, depending on whether recombination is through three-body or radiactive processes.

C. Superluminous Velocity of the Front

It is quite possible for an ionization or recombination front to move across a gas at or above the speed of light. For example,

the ionization front could be produced by a laser or electron beam sweeping across the gas (much as the trace in a cathode ray tube can move across the screen faster than c). It seems clear physically that reflection cannot occur at such a front, since, in the case of a receding recombination front, the incident electromagnetic wave pulse cannot catch up with the front, and in the case of an oncoming ionization front, a reflected pulse would be immediately caught by the front. What actually happens, in the latter case, is that there is no reflected wave, but two propagating waves are generated in the plasma, as will now be shown.

Since $U > c$ in this case, we shall work in the laboratory frame. The three normal modes in the stationary plasma are then the magnetic wave ($\omega_m^* = 0$), the rightward-propagating or evanescent (depending on whether $\omega_1^* > \omega_p$) wave,

$$k_1^*(\omega_1^*) = (\omega_1^*/c)(1-\omega_p^2/\omega_1^{*2})^{1/2} \tag{40a}$$

and the leftward-propagating or growing wave,

$$k_2^*(\omega_2) = -(\omega_2^*/c)(1-\omega_p^2/\omega_2^{*2})^{1/2}. \tag{40b}$$

Since the reflection problem is non-stationary in the laboratory frame, both k^* and ω^* for the transmitted waves can differ from the incident wave values. However, the continuity conditions at the front can be met only if all waves are in phase at the front ($z = -Ut$), i.e.

$$-k_i^* Ut - \omega_i^* t = -k^* Ut - \omega^* t \tag{41}$$

for each wave. [Applying this condition to the reflected wave is an alternate method of deriving the double Doppler shift for the subluminous case, Eq. (1).] Thus

$$-\omega_i^*(\beta+1) = -k_m^* U \tag{42a}$$

$$= -\omega_1^* \left[\beta\left(1 - \frac{\omega_p^2}{\omega_1^{*2}}\right)^{1/2} + 1\right] \tag{42b}$$

$$= \omega_2^* \left[\beta\left(1 - \frac{\omega_p^2}{\omega_2^{*2}}\right)^{1/2} - 1\right] , \tag{42c}$$

where $\beta \equiv U/c > 1$. Equations (42b,c) can be solved for ω_1^* and ω_2^*, with the result

$$\frac{\omega_1^*(z)}{\omega_i^*} = -\frac{1}{\beta-1} \mp \frac{\beta}{\beta-1}\left[1 + \frac{\beta-1}{\beta+1}\left(\frac{\omega_p}{\omega_i^*}\right)^2\right]^{1/2} \tag{43}$$

Thus ω_1^* and ω_2^* are both real, which implies that k_1^* and k_2^* are also real [from the phase-matching conditions (42b,c)]; it follows that neither wave is cut off, i.e. $\omega_p^2 < \omega_1^{*2}$ and $\omega_p^2 < \omega_2^{*2}$. Moreover one of the waves is rightward-propagating and the other is leftward-propagating (i.e. runs after the front, but never catches up with it). Thus the three amplitude-matching conditions discussed in Sec. IIA (continuity of E, B, and $\partial B/\partial z$) can be met by choosing the amplitudes of the three permissable plasma waves, with no

reflected wave (we omit the statement of the results here). The interpretation of the leftward propagating wave is that it is excited at the boundary and is then left behind by the front. It does not represent energy launched by a source at $z = +\infty$ and so the usual Sommerfield radiation condition does not apply.

III. Continuous Transition

We now consider an ionization or recombination front of arbitrary shape and width, but with $U < c$ and normal plane wave incidence from the gas. We work in the front frame, wherein the electron density $n(z)$ is stationary, and the plasma/gas streaming velocity U is constant in space and time. For the ionization front case ($U > 0$), the mean transverse velocity[18] of the electron fluid, $\underset{\sim}{y}(z,t)$, is determined by the momentum conservation equation,

$$nm_e\gamma \frac{\partial \underset{\sim}{y}}{\partial t} + m_e\gamma U \frac{\partial}{\partial z}(n\underset{\sim}{y})$$

$$\equiv nm_e\gamma\left(\frac{\partial \underset{\sim}{y}}{\partial t} + U\frac{\partial \underset{\sim}{y}}{\partial z}\right) + m_e\gamma U\underset{\sim}{y}\frac{dn}{dz} = -ne\left(\underset{\sim}{E} + \frac{1}{c}\underset{\sim}{U}x\underset{\sim}{B}\right). \qquad (44)$$

Ionization does not constitute a source of electron transverse momentum, since electrons are born with $\underset{\sim}{y} = 0$. Thus, as new electrons are born, they share in the local transverse electron momentum, thereby tending to reduce $\underset{\sim}{y}$. This is the interpretation of the term $m_e\gamma U\underset{\sim}{y}dn/dz$ on the left-hand side of Eq. (44). Using (44) and Maxwell's equations (8,9), and requiring that all quantities have the time dependence $\exp(-i\omega t)$ of the incident wave (since the medium is stationary in the front frame), we arrive at the following wave equation,

$$[c^2d^2/dz^2 + \omega^2 - \omega_p^2(z)](-i\omega + Ud/dz)E = 0. \tag{45}$$

The case of a recombination front is somewhat different. Since the transverse momentum of an electron is lost from the electron fluid when it recombines, a momentum sink $m\gamma\underset{\sim}{v}\rho(z)$ must be added to the right-hand side of the momentum equation, where $\rho \equiv Udn/dz$ is the local recombination rate. Thus the equation for $\underset{\sim}{v}$ becomes

$$nm_e\gamma\left(\frac{\partial \underset{\sim}{v}}{\partial t} + U\frac{\partial \underset{\sim}{v}}{\partial z}\right) = -ne(\underset{\sim}{E} + \frac{1}{c}\underset{\sim}{U} \times \underset{\sim}{B}). \tag{46}$$

Maxwell's equations and (46) lead to a different wave equation,

$$(-i\omega + Ud/dz)\omega_p^{-2}(c^2d^2/dz^2 + \omega^2 - \omega_p^2)E = 0, \tag{47}$$

for the recombination front case.

The recombination front case is most easily treated. Equation (47) can be immediately integrated once to yield

$$(c^2\frac{d^2}{dz^2} + \omega^2 - \omega_p^2)E = E_o\omega_p^2 \exp(i\omega z/U). \tag{48}$$

For large positive z, ω_p becomes constant and Eq. (48) possesses the following particular solution :

$$E_p = \omega_p^2 E_o[\omega^2(1-\beta^{-2})-\omega_p^2]^{-1} \exp i(\frac{\omega}{U} z),\ z \to +\infty. \tag{49}$$

However, for the recombination front case, $U < 0$ and (49) represents a

magnetic wave transporting energy in from $z = +\infty$. Since this is physically unacceptable, the constant E_o must be zero, and (48) reduces to the usual equation for wave propagation in a stationary plasma,

$$\left(\frac{d^2}{dz^2} + \frac{\omega^2-\omega_p^2}{c^2}\right) E = 0. \qquad (50)$$

Thus the problem of reflection from a receding recombination front is equivalent, in all respects, to reflection from a receding physically moving plasma with the same electron density profile (in the frame in which the profile is stationary). In the recombination front frame, the solution to (50), in the gas ($z \to -\infty$, $\omega_p \to 0$), is of the form

$$E(z) = E(e^{i\omega z/c} + \Gamma\, e^{-i\omega z/c}). \qquad (51)$$

Γ is the (amplitude) reflection coefficient for the stationary front in stationary plasma. It is given exactly by Eqs. (20) and (23) if the front happens to be abrupt (which means that its width is much less than a wavelength). It is also well known that $|\Gamma| = 1$ if the plasma is overdense. In other cases, the calculation of Γ is a well-known, but usually complicated, mathematical problem. In general, the reflected power in the front frame is given in terms of Γ by Eq. (32a), and the reflected power and pulse energy in the laboratory frame by Eqs. (33) and (34). The results of the previous section now become a special case, for which Γ is known exactly, of this general result.

We can also write down the general solution for the ionization front case, Eq. (45):

$$E = \int_{-\infty}^{z} dz' \, g(z') \exp\left[i\left(\frac{\omega}{U} - i\epsilon \right)(z-z') \right] , \qquad (52)$$

where $g(z)$ is a solution to the stationary medium reflection problem (50) with appropriate outgoing wave boundary conditions, and ϵ is a positive infinitesmal introduced for convergence ($\epsilon \to 0^+$). In writing (52), a particular solution $Ae^{i\,\omega/U\,z}$ which would appear on the right hand side has been neglected ($A = 0$), since $A \neq 0$ would imply the existence of a rightward-propagating magnetic wave component, $E \sim \exp(i\omega z/U)$, in the plasma-free region $z \to -\infty$, where the incoming wave is specified to be an electromagnetic wave of given amplitude, $E = E_i \exp(i\omega z/c)$.

We notice that to find the reflection coefficient, we need to evaluate Eq. (52) only asymptotically at $z \to -\infty$, and that to do this we only need the solution $g(z)$ of (50) asymptotically at $z \to -\infty$. But the latter is given by Eq. (51), in terms of the constant Γ (the reflection coefficient for the stationary problem). Substituting (51) in (52), we can perform the integration exactly, and find

$$E = E_i \left(e^{ikz} + \frac{1-\beta}{1+\beta} \Gamma e^{-ikz} \right) . \qquad (53)$$

The reflected power, in the front frame, is then

$$\frac{P_r}{P_i} = \left(\frac{1-\beta}{1+\beta} \right)^2 |\Gamma|^2 . \qquad (54)$$

It is thus generally true that the reflection coefficient (in the frame of a moving ionization front) is $(1-\beta)^2/(1+\beta)^2$ times the

reflection coefficient for a stationary plasma with the same density profile (and thus is always less than unity). The results of Sec. IIA are a special case of this conclusion. In particular, if $\omega^2 < \omega_p^2$, then $|\Gamma|^2 = 1$ and the reflection coefficient is independent of the exact profile $n(z)$!

Lorentz transforming to the laboratory frame, and following the same reasoning as in Sec. IIA, we find the reflected power and pulse energy to be

$$\frac{P_r^*}{P_i^*} = |\Gamma|^2, \tag{55}$$

$$\frac{\epsilon_r^*}{\epsilon_i^*} = \frac{1-\beta}{1+\beta} |\Gamma|^2 = \frac{\omega_i^*}{\omega_r^*} |\Gamma|^2 < 1. \tag{56}$$

B. Exact Solution for a Particular Profile

Having obtained a rather general result for the magnitude of the reflection coefficient, we now consider the excitation of the magnetic wave, discussed in Sec. II for the sharp boundary case. We shall find that the situation is radically different for the case of a sharp boundary and for the case of a broad transition many wavelengths thick. In order to illustrate this we consider a specific profile

$$\omega_p^2 (z) = \frac{1}{2} \omega_{po}^2 [1 + \tanh (z/2\sigma)], \tag{57}$$

and assume that $\omega_p^2(\infty) \equiv \omega_{po}^2 > \omega^2$, i.e. the plasma is overdense. The

exact solution $g(z)$ to Eq. (50), with this functional form for $\omega_p^2(z)$, is known in analytic form,[19] in terms of the hypergeometric function. By using the Barnes integral representation of the hypergeometric function, the expression for $g(z)$ in Ref. 19 may be written in the following form[19]:

$$g(z) = \frac{e^{-\alpha kz}}{2\pi i}\int_C ds \ \frac{\Gamma(A_1)\Gamma(A_2)\Gamma(1-s)\exp[z(1-s)/\sigma]}{\Gamma(s + 2k\sigma\alpha)}, \qquad (58)$$

where $A_{1,2} = (s-1 \mp ik\sigma + k\sigma\alpha)$, $\alpha = (\omega_{po}^2 - \omega^2)^{1/2}/\omega$, $\Gamma(w)$ are gamma functions, $g(z) \sim \exp(-\alpha kz)$ for large z/σ as required, and the contour C is illustrated in Fig. 2. Since $\Gamma(w)$ has no zeros and an infinite number of poles at $w = 0, -1, -2, \ldots$, with residues $(-1)^w/(-w)!$, the integrand of Eq. (58) has the poles labeled with x's in the figure. The series of poles on $\mathrm{Im}(s) = k\sigma$ and on $\mathrm{Im}(s) = -k\sigma$ result from $\Gamma(A_1)$ and $\Gamma(A_2)$ respectively; while the series of poles on the real axis result from $\Gamma(1-s)$. Putting (58) in (52) and interchanging the orders of the z' and s integrations, we obtain

$$E = \frac{\sigma e^{-k\alpha z}}{2\pi i}\int_C ds \ \frac{\Gamma(A_1)\Gamma(A_2)\Gamma(1-s)\exp[-(s-1)z/\sigma]}{\Gamma(s+2k\sigma\alpha)(s-1+k\sigma\alpha + i\omega\sigma/U)}. \qquad (59)$$

Thus another pole is introduced in the integrand at $s = 1-k\sigma\alpha - i\omega\sigma/U$ (labeled by a dot in Fig. 2). Note that the contour C lies to the left of this pole so that (as we shall see) E satisfies the condition of having no component proportional to $\exp(i\omega z/U)$ in the region $z \ll -\sigma$. For $z > 0$, the contour can be closed with a large semicircle at infinity in $\mathrm{Re}(s) > 0$. For $z \gg \sigma$ the dominant contribution is from the pole at $s = 1 - k\sigma\alpha + i\omega\sigma/U$, with all other pole contributions going exponentially to zero. Thus

$$E \cong X_3 \exp(i\omega z/U), \text{ for } z \gg \sigma, \tag{60a}$$

where X_3 is obtained from the residues at the pole. Similarly we obtain

$$E \cong X_1 e^{ikz} + X_2 e^{-ikz}, \text{ for } z \ll -\sigma, \tag{60b}$$

which results from the dominant pole contributions at $s = 1-k\sigma\alpha \pm ik\sigma$. Evaluating the residues, X_1, X_2 and X_3, we obtain the reflection coefficient $|X_2/X_1|^2 = (1-\beta)^2/(1+\beta)^2$, in accordance with the general result (54). We also find the excitation coefficient for the magnetic wave

$$\left|\frac{X_3}{X_1}\right|^2 = \frac{2\pi\beta^2}{\beta^2\alpha^2+1}\,\frac{1-\beta}{1+\beta}\left(\frac{\omega_{po}}{\omega}\right)^2 \frac{2k\sigma\,\sinh(2\pi k\sigma)}{\sinh[\pi k\sigma\,(1-\beta)/\beta]\sinh[\pi k\sigma(1+\beta)/\beta]}. \tag{61}$$

In obtaining (61) we have made use of the following gamma function identities: $|\Gamma(iy)|^2 = \pi[y\,\sinh(\pi y)]^{-1}$ (where y is real), $\Gamma(z+1) = z\Gamma(z)$, and $|\Gamma(z)|^2 = |\Gamma(z^*)|^2$ (where z^* is the conjugate of z). For $\sigma \to 0$, Eq. (61) yields the result for the sharp boundary case found in Sec. II. For $\sigma \to \infty$, the excitation coefficient for the magnetic wave becomes exponentially small. While we have demonstrated this only for a particular profile, this same result can be shown in a general way for a large class of profiles. This may be interpreted as follows: When a particle is suddenly ionized, its transverse velocity acquires an oscillatory component at the local frequency of the usual electromagnetic wave, and also a component which has zero frequency in

the laboratory frame (as discussed in Sec. II). For the case of a sharp front, this transverse streaming part created at the front sets up currents which support the magnetic wave. For the broad front, however, the transverse streaming velocity component of electrons is created continuously throughout the broad front. At any point behind the front there will be electrons born at different points in the front, having correspondingly different transverse velocities. The velocities of these electrons add with different phases to produce a reduced current, and when the front is very broad, this phase mixing results in an exponentially small magnetic wave.

The analyses of Sec. II and of the present section present us with the following puzzle. For the sharp boundary case we found (Sec. II) that the energy lost upon reflection was used to excite the magnetic wave. However, for the broad boundary case we have now shown that the excitation of the magnetic wave becomes exponentially small. Yet we have shown that the reflection coefficient is the same in both cases. In the next subsection we resolve this apparent inconsistency.

C. Energy Conservation for the Case of a Broad Ionization Front ($c > U > 0$)

As before we work in the front frame and attempt to demonstrate conservation of energy. The key point for the limit of a broad front is that even though there is no transmitted magnetic wave, energy is still transferred into the plasma by the phase mixed transverse streaming electron velocities- i.e. a transverse electron temperature is produced. As seen in the front frame, energy transfer also occurs through the plasma axial recoil velocity ΔU.

The conservation equations for axial momentum and energy are similar to those discussed in the sharp front case, Eqs. (35), except for the absence of the electromagnetic fluxes associated with the magnetic wave, i.e.

$$P_i+P_r = \Delta[nU^2(m_e\gamma_e+m_i\gamma_i)]$$

$$= \frac{1}{2} m_e n\gamma^3\beta^2 < v^2 > + (m_e+m_i)n\gamma^3 U\Delta U, \tag{62a}$$

$$cP_i-cP_r = \Delta[nUc^2(m_e\gamma_e+m_i\gamma_i)]$$

$$= \frac{1}{2} m_e nU\gamma^3 < v^2 > + (m_e+m_i)n\gamma^3 U^2\Delta U, \tag{62b}$$

where Δ again denotes the difference between the value of a quantity in the region $z \to +\infty$ with and without the presence of the incident electromagnetic wave [note that $\Delta(nU) = 0$]. Eliminating ΔU from (62) and using (54), we obtain the condition for energy conservation,

$$cP_i = \frac{1}{4} m_e n\gamma^3(1+\beta)^2 c < v^2 > . \tag{63}$$

It thus remains to verify that this energy conservation condition is indeed satisfied for the case of a broad front. To calculate $g(z)$, the solution of (50), for a very gradual transition, it is adequate to use the WKB approximation[7] for $g(z)$,

$$g(z) \cong A(1-\omega_p^2(z)/\omega^2)^{-1/4}[e^{i\psi} + e^{-i\psi + \theta}], \text{ if } \omega^2 > \omega_p^2(z), \tag{64}$$

$$g(z) \cong 0, \text{ if } \omega^2 \leq \omega_p^2(z), \tag{65}$$

where $\psi = ik\int^{z}\left\{1-[\omega_p(z')/\omega]^2\right\}^{1/2} dz'$ and θ is a constant phase factor. Using (64) and (65) in (52), we have $[\omega^2 > \omega_p^2(z)]$

$$E \cong \frac{A}{\left(1-\frac{\omega_p^2}{\omega^2}\right)^{1/4}}\left[\frac{(1-\beta)e^{i\psi}}{1-\beta\left(1-\frac{\omega_p^2}{\omega^2}\right)^{1/2}}e + \frac{1-\beta}{1+\beta\left(1-\frac{\omega_p^2}{\omega^2}\right)^{1/2}}e^{-i\psi+i\theta}\right] \quad (66)$$

The transverse velocity of an electron created at time t and position z can be regarded as the sum of a streaming component (zero frequency in the laboratory frame) and an oscillating component; the total electron transverse velocity at the instant of ionization must be zero. By integrating the transverse acceleration due to both the incident and reflected waves, we can calculate the transverse streaming velocity component; we then find

$$m_e n\gamma^3 \langle v^2 \rangle = m_e\gamma^3 \left|\frac{eA}{m\omega\gamma}\right|^2(1-\beta^2)\int_{-\infty}^{z_o}[1-\omega_p^2(z)/\omega^2]^{-1/2} \quad (67)$$

$$\left\{[1-\beta(1-\omega_p^2(z)/\omega^2)^{1/2}]^{-2} + [1+\beta(1-\omega_p^2(z)/\omega^2)^{1/2}]^{-2}\right\}(dn(z)/dz)dz,$$

where z_o is defined by $\omega_p^2(z_o) = \omega^2$. Making a change of integration variable from z to $W \equiv (1-\omega_p^2(z)/\omega^2)^{1/2}$, we readily obtain

$$\frac{1}{4} m_e n\gamma^3(1+\beta)^2 c \langle v^2 \rangle = \frac{|A|^2}{4\pi} c, \quad (68)$$

which is the same as cP_i, completing the proof.

IV. Cases of Oblique Wave Incidence and Incidence in a Waveguide

If the incident wave propagates obliquely to an infinite planar ionization front, or if the waves and plasma are confined within a waveguide, the waves have a perpendicular component $k_\perp$ of the propagation vector. In this section, we extend the results of the previous section by including $k_\perp$ in the calculation. We consider only the case where $\underset{\sim}{E}$ is transverse to the electron density gradient ∇n_e, i.e. $\underset{\sim}{E}$ is perpendicular to the plane of incidence for the oblique incidence case, or the incident mode is a transverse electric (TE) mode in the waveguide case. The other polarization leads to the well-known complications of resonant absorption (e.g. excitation of electrostatic Langmuir waves) even for $\underset{\sim}{U} = 0$, and is presently under study.

Again working in the front frame, from Maxwell's curl $\underset{\sim}{E}$ equation, $\underset{\sim}{U} \times \underset{\sim}{B}/c = i\omega^{-1} U d\underset{\sim}{E}/dz$. Also from Maxwell's equations we have

$$(d^2/dz^2 + \omega^2/c^2 - k_\perp^2)\underset{\sim}{E} = 4\pi n e \partial \underset{\sim}{v}/\partial t. \tag{69}$$

Here $k_\perp = (\omega_i^*/c) \sin \theta_i^*$ for the obliquely incident plane wave case, with θ_i^* the angle of incidence (in the laboratory frame). For the waveguide case, $k_\perp$ is the usual waveguide mode transverse component, e.g. $k_\perp^2 = (p\pi/a)^2 + (q\pi/b)^2$ for the pq mode of a rectangular a by b waveguide. Using these equations together with (44) yields

$$(-i\omega + U d/dz)\omega_p^{-2} (c^2 d^2/dz^2 + \omega^2 - \omega_p^2 - k_\perp^2 c^2)E = 0 \tag{70}$$

for the recombination front case, and

$$(c^2d^2/dz^2 + \omega^2 - \omega_p^2 - k_\perp{}^2c^2)(-i\omega + Ud/dz)E = 0 \qquad (71)$$

for the ionization front case. These equations differ from Eqs. (45,47) only by the inclusion of the $k_\perp^2c^2$ term. Following the reasoning used in Sec. III, we again find that the recombination front reflection coefficient (in the front frame) is the same as for a stationary front ($U = 0$), i.e.

$$E(z \to -\infty) = E_i(e^{ik_z z} + \Gamma e^{-ik_z z}) \qquad (72)$$

where Γ is again the reflection coefficient for a stationary front ($U = 0$). For the ionization front, we find, similarly to Eq. (53),

$$E(z \to -\infty) = E_i(e^{ik_z z} + \frac{1-k_zU/\omega}{1+k_zU/\omega}\Gamma e^{-ik_z z}), \qquad (73)$$

where ω and k_z are the frequency and z-component of the wave number in the front frame.

Lorentz transformation to the laboratory frame shows that the ratio of reflected to incident frequencies can be written in any of the three equivalent forms

$$\frac{\omega_r^*}{\omega_i^*} = \frac{1+k_zU/\omega}{1-k_zU/\omega} \qquad (74a)$$

$$= \frac{1+\beta\cos\theta_i^*}{1-\beta\cos\theta_r^*} \qquad (74b)$$

$$= \frac{1+2\beta\cos\theta_i^*+\beta^2}{1-\beta^2}, \qquad (74c)$$

where θ_i^* and θ_r^* are the angles of incidence and reflection in the laboratory frame. Equations (74a) and (74b) exhibit admirable symmetry, but only (74c) is completely defined in terms of incident wave parameters. Thus Eqs. (74) can also be used to solve explicitly for k_z and θ_r^*.

It follows from Eqs. (72)-(74a) that the ratio of incident to reflected power, in the front frame, is

$$P_r/P_i = |\Gamma|^2 \tag{75}$$

for a recombination front, and

$$P_r/P_i = (\omega_i^*/\omega_r^*)^2|\Gamma|^2 \tag{76}$$

for an ionization front. As in Secs. II and III, we find the ratio of reflected wave packet energy ϵ_r^* to incident packet energy ϵ_i^*, in the laboratory frame, by using Eqs. (74-76) and arguing that wave action, i.e. number of photons, is a Lorentz invariant, so that $\epsilon_i/\omega_i = \epsilon_i^*/\omega_i^*$ and $\epsilon_r/\omega_r = \epsilon_r^*/\omega_r^*$. We then find

$$\frac{\epsilon_r^*}{\epsilon_i^*} = \frac{\omega_r}{\omega_i}|\Gamma|^2 \tag{77}$$

for a recombination front, and

$$\frac{\epsilon_r^*}{\epsilon_i^*} = \frac{\omega_i}{\omega_r}|\Gamma|^2 \tag{78}$$

for an ionization front. Equations (75-78) are identical to the results for normally incident plane waves, and the Doppler shift (74) differs only in the substitution of k_z for k.

All of these results apply to both the obliquely incident plane wave on an infinite planar front, and to incidence in a waveguide. However, the power reflection coefficient in the laboratory frame is different in the two cases, since

$$P_r^*/P_i^* = (\varepsilon_r^*/\tau_r^*)/(\varepsilon_i^*/\tau_i^*), \tag{79}$$

and the pulse length τ^* depends on the group velocity, which differs in the two cases. For the case of oblique incidence in free space, the group velocity equals the phase velocity,

$$\tau_i^*/\tau_r^* = \omega_r^*/\omega_i^*, \tag{80}$$

and

$$\frac{P_r^*}{P_i^*} = \frac{\omega_i}{\omega_r}\,\frac{\varepsilon_r^*}{\varepsilon_i^*}\ , \tag{81}$$

just as in Secs. II and III. However for a waveguide,

$$\tau_i^*/\tau_r^* = (\beta_{gs}-\beta)/(\beta+\beta_g), \tag{82}$$

where[3]

$$\beta_g = (1 - k_\perp^2 c^2/\omega_i^{*2})^{1/2} \tag{83}$$

and

$$\beta_{gs} = \beta_g\,\frac{1+\beta^2 + 2\beta\beta_g^{-1}}{1+\beta^2 + 2\beta\beta_g}\ . \tag{84}$$

V. Critique of Previous Work: Moving Interface Between Dielectrics

A considerable (but rather disjointed) theoretical literature exists on reflection and transmission of electromagnetic waves at moving discontinuities in electrodynamic properties of media.[8-15] Although many of the authors have argued that their calculations apply to moving ionization fronts, the existence of the magnetic wave is overlooked in almost all of these works.[8-10,12-15] Consequently the boundary value problem which is set up, and the resulting solutions, are incorrect when applied to plasma ionization fronts, as will be discussed below in some detail. We note that the sharply discontinuous moving ionization front problem has been addressed correctly by Hughes and coworkers.[11] However, these authors were interested in non-relativistic shocks, and therefore neglected to calculate the reflection coefficient, which differs from unity only by terms of order β (and constitutes our principal result). Hughes, et al.,[11] also considered the different situation of a collision-dominated plasma with collision frequency large compared to the wave and plasma frequencies.

Of the remaining calculations in the literature, several set up the problem of reflection/transmission at a moving discontinuity in dielectric coefficient. Since a strictly dielectric formulation is used, it is implicitly assumed that the medium, like a vacuum, sustains only two transverse modes at any given frequency, and the possibility of a third mode (i.e. the magnetic mode in a plasma) is excluded. We shall consider in some detail the model of Tsai and Auld,[12] wherein the moving interface is treated as a sharp moving discontinuity between stationary

dispersionless materials with different dielectric constant, i.e. it is assumed that, within each region, the polarization $\underset{\sim}{P}(\underset{\sim}{x},t)$ is proportional to the local electric field $\underset{\sim}{E}(\underset{\sim}{x},t)$,

$$\underset{\sim}{P}(\underset{\sim}{x},t) = \chi \underset{\sim}{E}(\underset{\sim}{x},t), \tag{85}$$

at all points. Under these assumptions, and for normal incidence, it is found[12] that the Doppler shift of the reflected wave is

$$\frac{\omega_r^*}{\omega_i^*} = \frac{1+U/V_{pi}}{1-U/V_{pi}}, \tag{86}$$

the pulse length is reduced as

$$\frac{\tau_r^*}{\tau_i^*} = \frac{\omega_i^*}{\omega_r^*}, \tag{87}$$

the power reflection coefficient is

$$\frac{P_r^*}{P_i^*} = \left(\frac{\omega_r^*}{\omega_i^*}\ \frac{1-(\epsilon_2/\epsilon_1)^{1/2}}{1+(\epsilon_2/\epsilon_1)^{1/2}}\right)^2, \tag{88}$$

and the reflection coefficient for total pulse energy is

$$\frac{\epsilon_r^*}{\epsilon_i^*} = \frac{\omega_r^*}{\omega_i^*}\left(\frac{1-(\epsilon_2/\epsilon_1)^{1/2}}{1+(\epsilon_2/\epsilon_1)^{1/2}}\right)^2, \tag{89}$$

where V_{pi} is the phase velocity of the incident wave, and ϵ_1 and ϵ_2 are the dielectric coefficients on the two sides of the interface.

We see immediately that if $V_{pi} \to c$, i.e. the dielectric susceptibility is weak on the incident side, and ϵ_2 is associated with the plasma dielectric, $1-\omega_p^2/\omega^2$, Eqs. (86-89) become identical to Eqs. (1-4) for the reflection off the front of a moving plasma. In particular, Eqs. (86) and (89) indicate that the energy of the reflected wave pulse may exceed that of the incident wave pulse, even though the dielectric material is not moving. This reflection process is thus unlike the process of reflection off a moving ionization front in a stationary plasma for which we have seen that $\epsilon_r^* \leq \epsilon_i^*$ always holds. One may reasonably wonder about the reasons for this difference, and the source of the extra reflected energy in the case of the dielectric interface. We shall not perform a complete calculation of the latter, but we hope that the following comments will help to clarify these points.

There are in reality no completely dispersionless dielectrics that always obey Eq. (85). Any dielectric may be considered as a collection of oscillators, with natural resonances at one or more frequencies. Let ω_o (a spatially dependent quantity) be the lowest such resonance. Then a number of tacit assumptions are built into the dielectric discontinuity model of Ref. 12:

(a) If σ is the width of the transition region, then σ is much less than the incident and reflected wavelengths, since a sharp transition is assumed.

(b) The wave frequency ω_i^* at any given point is much less than the local value of ω_o, since it is assumed that the dispersionless relation (85) holds, i.e. that the dielectric responds to the wave

field as if it were a time-independent field.

(c) It is also assumed that

$$\sigma \gg U\omega_o^{-1}, \tag{90}$$

since this is the requirement for the change in dielectric coefficient to be adiabatic, so that Eq. (85) is obeyed near the interface. Thus the interface cannot be a strict discontinuity. For example, let us consider the simplest possible model of a dielectric: a collection of identical classical oscillators, with electrons attached to atoms by "springs". Each oscillator then obeys the equation

$$\ddot{x} = -\omega_o^2 x - eE/m_e. \tag{91}$$

If we let E be constant [in accordance with assumption (a) discussed above], but allow ω_o to vary in time, as the front passes over a given atom, then

$$x \approx -eE/m_e\omega_o^2 \tag{92}$$

if Eq. (90) holds; this then allows (85) to be satisfied. In the opposite limit to Eq. (90), e.g. in the case of an abrupt transition from $\omega_o = \infty$ (tightly bound electrons - zero susceptibility) to finite ω_o,

$$\ddot{x} \approx -eE/m_e \tag{93}$$

in the immediate vicinity of the interface, i.e. the electrons act as if they were free. Thus this case corresponds microscopically (within the region $U\omega_o^{-1}$ from the front) to an abrupt ionization front, not to a discontinuity in dispersionless dielectrics.

(d) It is clear from these arguments that for the model of Ref. 12 to hold, <u>each individual</u> oscillator must make a smooth transition in accordance with Eq. (90). It is not sufficient for the macroscopic dielectric coefficient to change smoothly, as a result of a statistical distribution of many oscillators, each of which makes a sharp transition.

The fact that the reflected energy can exceed the incident wave energy, according to the dispersionless dielectric discontinuity model of Ref. 12, can be explained as follows. When the oscillator frequencies are changed adiabatically, in presence of an electric field (due to the waves), work is done on the oscillator by the mechanism that changes its frequency. Thus this energy is available to enhance the reflected wave. On the other hand, no work is done in suddenly changing the oscillator frequency. These results can be established by appropriately integrating Eq. (91), or by the following simple argument. Imagine an electron attached by a spring to an atom, in the presence of an electric field. If the spring is slowly released, work is done against the electric field. But if the electron is initially tied down by a string, no work is done in cutting the string, i.e. instantaneously increasing the susceptibility.

Thus, if one expects to apply the dispersionless dielectric

discontinuity model to a given experiment, one must verify that assumptions (a-d) are valid. In particular, one must pay attention to assumption (d), which deals with the microscopic physics.

VI. Applications

We have shown that the power reflection coefficient for upshifted microwaves reflected off an oncoming overdense ionization front is ideally unity. However, the reflected pulse is shortened as in Eq. (2); the total reflected wave packet energy, $\epsilon_r^* = (\omega_i^*/\omega_r^*)\epsilon_i^*$, is less than the incident energy and unfortunately decreases as the Doppler upshift increases.

Nevertheless, upshifting high-power microwave sources by factors of 10 to 100, with efficiency of 10% to 1%, could produce very interesting fluxes in the millimeter and particularly the submillimeter wavelength regimes, where intense sources have been hard to come by. This is particularly true if a clean, precisely controllable moving ionization front can be produced without an energy investment that far exceeds the energy of the microwave sources. This may well be possible, since the ionization energy which must be supplied to form an overdense plasma is quite modest, typically of the order of 0.1 joule per meter for a 10cm diameter plasma at $n_e = 10^{14}cm^{-3}$.

Many techniques for producing moving ionization fronts may be envisioned. A high current, relativistic electron beam propagating through a gas typically creates a moving ionized region in the stationary gas, with electron density much higher than that of the beam itself. It is also possible to drive a strong electromagnetic pulse down a gas-filled guide, producing an ionization front

accompanying the pulse. Perhaps the most promising approach for our purposes is to sweep an ionizing laser beam across the gas transversely. In fact, a variation of this approach has recently been demonstrated in connection with work on the ionization front ion accelerator. In this scheme, a precisely programmed sequence of laser pulses is fired (from a series of many light pipes) across a cylinder of gas. The laser frequency is tuned to excite the gas, which is then ionized by another laser propagating axially in the continuous wave mode.

One possible limitation on the microwave power that can be handled, in an ionization front reflector, would arise from the requirement that the incident microwaves themselves do not pre-ionize the gas. Thus a careful selection of the working gas and ionization mechanism may be necessary to optimize such a system.

VII. Summary and Conclusion

In this paper we have considered the problem of reflection of an incident electromagnetic wave from a relativistic oncoming ionization front or receding recombination front, where the front region is assumed to separate regions of stationary neutral gas and ionized plasma. We first considered the case of a normally incident plane wave on a sharp front, and obtained the following results:

(1) The reflection coefficient for energies in the incident and reflected wave pulses is $\epsilon_r^*/\epsilon_i^* = (\omega_i^*/\omega_r^*)|\Gamma|^2$ for the oncoming ionization front, and $\epsilon_r^*/\epsilon_i^* = (\omega_r^*/\omega_i^*)|\Gamma|^2$ for the recombination front case, where $|\Gamma|^2 = 1$ when the plasma is overdense [cf. Eqs. (28) and (33)].

(2) The duration of the reflected pulse is shortened (lengthened) for the ionization (recombination) front case, so that $\tau_r^*/\tau_i^* = \omega_i^*/\omega_r^*$, and the power reflection coefficients are $P_r^*/P_i^* = |\Gamma|^2$ for the ionization front, and $P_r^*/P_i^* = (\omega_r^*/\omega_i^*)|\Gamma|^2$ for the recombination front [cf. Eqs. (29) and (34)].

(3) Energy conservation was verified. In particular, for the ionization front in the overdense case ($|\Gamma|^2 = 1$), it was shown that the energy loss upon reflection was due to the excitation of a "magnetic wave" in the plasma region. The existence of this wave seems to have gone unrecognized until now.

We next considered a front with an <u>arbitrary</u> electron density profile. We found that conclusions (1) and (2) remain valid even in this more general situation. Point (3) however was found to be altered:

(4) As the thickness of the front increases the excitation coefficient of the magnetic wave decreases due to phase mixing of the transverse currents. This phase mixing leads to a type of collisionless heating in which the transverse temperature of the electron fluid is increased downstream from the ionization front.

For oblique incidence and incidence in a waveguide with $\underset{\sim}{E}$ transverse to the electron density gradient, conclusion (1) was again found to hold. However, for the waveguide case (2) no longer applies, since

$\tau_r^*/\tau_i^* \neq \omega_i^*/\omega_r^*$.

Acknowledgments

We are grateful to Dr. Thomas Antonsen and Dr. Wallace M. Manheimer for valuable contributions to the work. We also wish to acknowledge valuable discussions with Dr. Ira Bernstein, Dr. Jay Hirschfield, Dr. Selig Kainer, Dr. Robert Cawley, Dr. Walter Aron, and Dr. Conrad Longmire.

This work was supported by Naval Surface Weapons Center.

References

1. W. Pauli, "Theory of Relativity" (Pergamon Press, Inc., New York, 1958).
2. Asterisks will be used throughout the paper to denote quantities in the laboratory frame. Many calculations will be performed in the "front frame", defined in Sec. IIA, for which asterisks are not used.
3. V. L. Granatstein, P. Sprangle, R. K. Parker, J. Pasour, L. Sefter, M. Herndon and S. P. Schlesinger, Phys. Rev. A14, 1194 (1976).
4. In practice it is difficult to make a beam overdense, so that the wave is cut off in the absence of an axial magnetic field. In the presence of a B_z, however, a cut-off band occurs near the cyclotron frequency.
5. Proceedings of the Second International Conference on Submillimeter Waves, sponsored by IEEE, San Juan, Dec. 1976, to be published in IEEE Transactions on Microwave Theory and Technique, June 1977.
6. M. Lampe, E. Ott, W. Manheimer, and S. Kainer, IEEE Transactions on Microwave Theory and Technique, June 1977, to be published.
7. K. G. Budden, "Radio Waves in the Ionosphere" (Cambridge Univ. Press, 1961), Chap. 9.
8. F. B. Knox, J. Atmospheric and Terrestrial Phys. 24, 1003 (1962).
9. S. N. Stolyarov, Sov. Phys. - Tech. Phys. 8, 418 (1963).
10. A. M. Glutsyuk, Sov. Phys. - Tech. Phys. 9, 1042 (1965).

11. W. F. Hughes and F. J. Young, J. Fluid Mech. 19, 11 (1964); C. P. Chen and W. F. Hughes, J. Geophys. Res. 22, 6021(1967).

12. C. S. Tsai and B. A. Auld, J. Appl. Phys. 38, 2106 (1967).

13. J. Ramasastry and G. Y. Chin, Electronics Letters 3, 479 (1967).

14. H. Fujita and H. Muramatsu, Proceedings IEEE 56, 1605 (1968); H. Fujita and T. Yanase, Electronics and Communications in Japan 52B, 78 (1969).

15. C. L. Sam, D. W. Faries and H. J. Gerritsen, Phys. Letters 34A, 429 (1971).

16. There is actually a small recoil in the flow velocity, but it is second order in the wave amplitude, and also first order in the ratio of electron to ion mass. This will be discussed in Sec. IIB.

17. This argument implicity assumes that the electromagnetic wave is non-dispersive, so that the group velocity is c. This holds in free space, but not in a waveguide (see Sec. IV).

18. In general, there is a spread in electron transverse velocities at any given point z at time t, since the velocity of a particular electron depends not only on the wave fields, but also on where and when that electron was ionized. The quantity of interest is the mean transverse velocity v(z,t) of the electron fluid, which determines the current density.

19. Op. cit. Ref. 7, pp. 370-380.

20. C. L. Olson, J. P. VanDevender, J. S. Pearlman, and A. Owyoung, Bull. Am. Phys. Soc. 21, 1183 (1976).

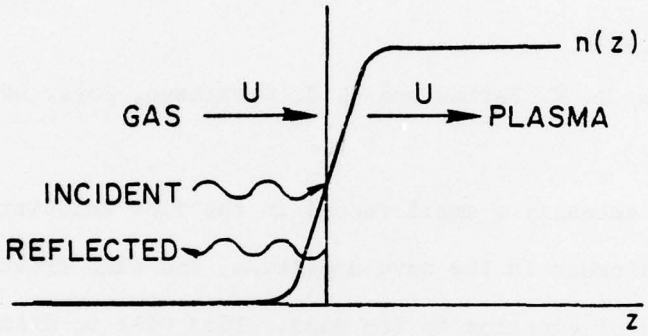

Fig. 1 — The scattering problem in the frame of reference of the front

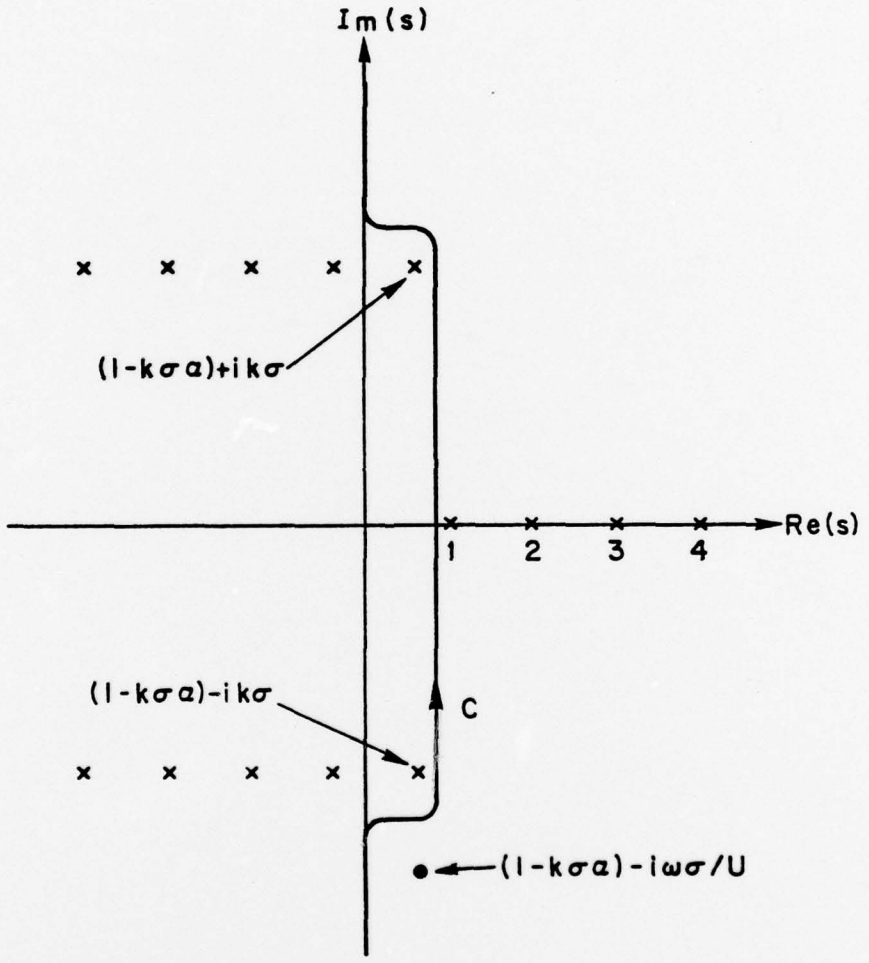

Fig. 2 — Integration path C for integrals in Eqs. (58) and (59). Poles of the integrand of (58) are denoted by x. The integrand of (59) has the same poles as that of (58) but with an additional pole at $s = 1-k\sigma\alpha - i\omega\sigma/U$, denoted by a dot on the figure.

Distribution List

Code 7000	
Code 7700	25 copies
Code 7740	
J. Pasour	1 copy
R. Parker	1 copy
V. Granatstein	1 copy
T. Godlove	1 copy
J. Siambis	1 copy
M. Friedman	1 copy
Code 7750	
V. Grishkot	150 copies
P. Sprangle	1 copy
W. Manheimer	1 copy
K. Papadopoulos	1 copy
D. Book	1 copy
S. Ossakow	1 copy
I. Haber	1 copy
T. Antonsen	1 copy
R. Lee	1 copy
P. Palmadesso	1 copy
S. Fisher	1 copy
K. R. Chu	1 copy
A. Drobot	1 copy
H. Bloomberg	1 copy
B. Hui	1 copy
E. Hyman	1 copy
Code 4000	1 copy
Code 5200	1 copy
Code 5203	1 copy
Code 5240	1 copy
Code 5242	1 copy
Code 5750	1 copy
Code 5740	1 copy
Code 5743A	1 copy
Code 5730	1 copy
Code 4120	1 copy
Code 5333	1 copy

Mr. Mark Baird
Hughes Research Laboratory
3011 Malibu Canyon Road
Malibu, Calif. 90265

Mr. Paul Fisher
AMSL-TI-BM
U. S. Army Electronics Command
Ft. Monmouth, N. J. 07703

Prof. G. Benford
Prof. C. W. Roberson
Prof. N. Rynn
Prof. Norman Rostoker
Department of Physics
University of California
Irvine, Calif. 92664

Prof. Edward Ott — 50 copies
Dr. Ravi Sudan
Dr. John Nation — Prof. B. Kusse
Prof. Peter Auer — Prof. C. Wharton
Dr. Hans Fleischman
Cornell University
Ithaca, New York 14850

Dr. A. Mondelli
Dr. Peter Korn
Maxwell Laboratories, Inc.
9244 Balboa Avenue
San Diego, Calif. 92123

Prof. S. P. Schlesinger
Prof. Thomas Marshall
Prof. Paul Diament
Department of Electrical Engineering and
Computer Sciences
Columbia University
New York, New York 10027

Prof. Robert Gross
Laboratory of Plasma Physics
School of Engineering
Columbia University
New York, N. Y. 10027

Dr. Howard Jory
Varian Associates
611 Hansen Way
Palo Alto, Calif. 94303

Dr. W. Gardner
Mr. Frank E. Welker
Rome Air Development Center
(OCTM-3)
Rome, New York 13440

Dr. Herbert A. Dropkin
Harry Diamond Laboratories
Washington, D. C. 20438

Commander Hugo A. Hardt
Naval Air Systems Command (AIR-03PB)
Department of the Navy
Washington, D. C. 20350

Prof. Enrico Levi
Polytechnic Institute of New York
Department of Electrophysics
Farmingdale, Long Island, N.Y. 11735

Dr. W. Holt
Dr. R. Wasneski
Mr. J. Shuler
Naval Weapons Laboratory
Dahlgren, VA 22448

Prof. Ira Bernstein
Prof. J. L. Hirschfield
Yale University
Mason Lab
400 Temple Street
New Haven, Conn. 06520

Prof. G. Bekefi, Rm. 36-213
Research Laboratory of Electronics
M.I.T.
Cambridge, Mass. 02139

Prof. Kun Mo Chung
Department of Electrical Engineering
Polytechnic Institute of New York
Route 110
Farmingdale, N. Y. 11735

Dr. S. J. Buchsbaum
Bell Telephone Laboratories
Holmdell, N. J. 07733

Dr. Felix Dothan
Hebrew University
Department of Physics
Jerusalem, Israel

R. W. Laton, Group 33
Mail Stop C-380
Lincoln Labs
P. O. Box 73
Lexington, Mass. 02173

George McMaster
Raytheon Company
Foundry Avenue
Waltham, Mass. 02154

Dr. John Madey
Department of Physics
Stanford University
Stanford, Calif. 94305

Prof. R. H. Pantell
Department of Electrical Engineering
Stanford University
Stanford, California 94305

Prof. Norman M. Kroll
Department of Physics
University of California
San Diego, La Jolla, Calif. 92038

Prof. Wolfgang Panofsky
SLAC
P. O. Box 4349
Stanford, Calif. 94305

Dr. John F. Vesecky (Theory)
Astronomy Department
The University
Leicester LE1 7RH
ENGLAND
(No need to use AIR MAIL if it
gets expensive)

Dr. David L. Judd
LBL
University of California
Berkeley, Calif. 94720

Tomas Hirschfeld
Block Engineering
19 Blackstone Street
Cambridge, Mass. 02139

Claude Elbaz, Scientific Attache
Ambassade de France Aux Etats Unis
2129 Wyoming Avenue, N.W.
Washington, D. C. 20008

Dr. Akira Hasegawa
Bell Telephone Labs.
Murray Hill, New Jersey

Lawrence Livermore Laboratory
Livermore, California 94550

R. J. Briggs
R. Buntzen
T. J. Fessenden
R. E. Hester
H. W. Kruger
E. P. Lee
V. K. Neil
L. D. Pearlstein

Naval Surface Weapons Center
White Oak
Silver Spring, Maryland 20910

C. Huddleston
R. Haislmaier
M. Brown
D. Simons
R. Biegalski
J. Pastine
K. Enkenhus

G. Hudson
R. Cawley

Ballistics Research Lab
Aberdeen Proving Grounds
Aberdeen, Maryland

D. Eccleshall
J. Batteh
J. Temperley

J. E. Leiss
National Bureau of Standards
301 Connecticut & Van Ness
Washington, D. C. 20234

C. F. Sharn
Naval Sea Systems Command
Washington, D. C. 20360

M. Halling
Naval Undersea Center
San Diego, California 92132

D. W. Padgett
Office of Naval Research
Navy Department
Arlington, Virginia 22217

E. H. Weinberg
Office of Naval Research
Navy Department
Arlington, Virginia 22217

S. Koslov
Office of the Assistant
Secretary of the Navy
Department of the Navy
Washington, D. C. 20350

W. Coleman
R. M. Dowe, Jr.
L. A. Kull
M. P. Fricke
R. Shanny
Science Applications, Inc.
P. O. Box 2351
1250 Prospect Street
La Jolla, California 92037

S. V. Yadavalli
Stanford Research Institute
333 Ravenwood Avenue
Menlo Park, California 94025

Simon Kassel
The Rand Corporation
2100 M Street
Washington, D. C. 20037

D. Gale
United States E.R.D.A.
Division of Military Applications
Room C-308, Mail Station A368
Washington, D. C. 20375

Lee O. Webster
BMD ATC-T
Box 1500
Huntsville, Alabama 35807

Dr. S. P. Gary
Dr. G. Vahala
The College of William and Mary in Virginia
Department of Physics
Williamsburg, VA 23185

R. R. Johnston
W. Aron
Science Applications, Inc.
P. O. Box 10286
2680 Hanover St.
Palo Alto, California 94303

Dr. J. Benford
Dr. Bailey
Dr. S. Putnam
Dr. S. Stallings
Dr. T. Young
Physics International Corporation
2400 Merced Street
San Leandro, California 94577

Dr. L. Thode
Dr. B. Godfrey
Los Alamos Scientific Laboratory
Los Alamos, New Mexico 87544

Dr. A. Toepfer
Dr. G. Yonas
Dr. P. Van Devender
Sandia Laboratories
Albuquerque, New Mexico 87115

Prof. A. N. Kaufman
Prof. C. McKee
University of California
Physics Department
Berkeley, California 94720

Dr. W. E. Drummond
Dr. J. R. Thompson
Austin Research Associated
600 W. 28th St.
Austin, Texas 78705

Dr. T. M. O'Neil
Dr. J. H. Winfrey
University of California, San Diego
Physics Department
La Jolla, California 92037

Prof. M. Reiser
Prof. R. C. Davidson
Prof. J. Guillory
Dr. Paulett Liewer
University of Maryland
Dept. of Physics and Astronomy
College Park, Maryland 20742

Dr. Yu I. Abrashitov
Dr. A. T. Altyntsev
Institute of Nuclear Physics
Siberian Branch, USSR Academy of Sciences
USSR

Dr. Melvin Goldstein
Goddard Space Flight Center
Greenbelt, Maryland 20771

Dr. J. M. Buzzi
Laboratoire PMI
Ecole Polytechnique
Plateau Palaiseau, 91120
Palaiseau, FRANCE

Professor H. Doucet
Laboratoire P M I
Ecole Polytechnique
Plateau Palaiseau, 91120
Palaiseau, FRANCE

Dr. S. Schneider
26628 Fond du Lac Rd
Palos Verdes Peninsula, CA 90274

Dr. Richard Spitzer
Stanford Linear Accelerator Center
P. O. Box 4349
Stanford, Calif. 94305

Professor John Walsh
Physics Department
Dartmouth College
Hanover, New Hampshire 03755

Academician A. V. Gaponov
Physical Technical Institute
Gorky State University
Gorky, USSR